MODELING OF A SANDWICH BEAM WITH THICKNESS-SHEAR ACTIVE-PASSIVE PIEZOELECTRIC NETWORKS

Heinsten Frederich Leal dos Santos, hfleal@sc.usp.br
Marcelo Areias Trindade, trindade@sc.usp.br
Department of Mechanical Engineering, São Carlos School of Engineering, University of São Paulo, Av. Trabalhador São-Carlense, 400, São Carlos, SP, 13566-590, Brazil.

Abstract. *Piezoelectric materials have been widely used as sensors and actuators for structural vibration control. Recently an active-passive damping technique, so-called Active Passive Piezoelectric Networks (APPN), was proposed by integrating an active voltage source with a passive resistance-inductance shunt circuit to a piezoeletric sensor/actuator. This technique allows to simultaneously dissipate passively vibratory energy through the shunt circuit and actively control the structural vibrations. This work presents the modeling of sandwich structures with extension and thickness-shear piezoelectric sensors/actuators connected to APPN. The model is based on a stress-voltage electromechanical model for the piezoelectric materials fully coupled to the APPN active-passive circuit. To this end, the APPN circuit equations are also included in the variational formulation. Hence, conservation of charge and full electromechanical coupling are guaranteed. The formulation results in a coupled finite element model with mechanical (displacements) and electrical (electrodes charges) degrees of freedom. An analysis of the resulting equations of motion is performed to identify the damping mechanisms provided by an active-passive piezoelectric network. A preliminary numerical analysis has shown that both extension and shear APPN configurations can be very interesting since the passive damping can be combined with the increase of active control authority.*

Keywords: *Vibration Control, Piezoelectric Materials, Active-Passive Piezoelectric Networks, Shear Piezoelectric Actuators, Sandwich Structures*

1. INTRODUCTION

Due to their strong electromechanical coupling, piezoelectric materials have been widely used as sensors and actuators for structural vibration control. They can be used either as actuators connected to an appropriate control law to provide active vibration control or as sensors connected to shunt circuits to provide passive damping. In the last decade, research was redirected to combined active and passive vibration control techniques. One of these techniques, so-called Active-Passive Piezoelectric Networks (APPN), integrates an active voltage source with a passive resistance-inductance shunt circuit to a piezoelectric sensor/actuator (Tsai and Wang, 1999). In this case, the piezoelectric material serves two purposes. First, the vibration strain energy of the structure can be transferred to the shunt circuit, through the difference of electric potential induced in the piezoelectric material electrodes, and then passively dissipated in the electric components of the shunt circuit (Forward, 1979; Hagood and von Flotow, 1991). On the other hand, the piezoelectric material may also serve as an actuator for which a control voltage can be applied to actively control the structural vibrations. This active mechanism combined to a velocity feedback, for instance, may then induce an additional active damping in the structure.

There are still some unresolved issues concerning this active-passive damping mechanism such as for which conditions simultaneous active-passive damping outperforms separate active and passive mechanisms, that is, whether the control voltage should be part of the shunt circuit or not (Thornburgh and Chattopadhyay, 2003). It has been shown that combined active-passive vibration control allows better performance with smaller cost than separate active and passive control, provided the simultaneous action is optimized (Tsai and Wang, 1999). On the other hand, like for purely passive passive shunted piezoelectric damping, most of the studies concerning APPN focus on the optimization of the electric circuit architecture and components. It is well-known however that the performance of both active and passive damping mechanisms is highly dependent on the effective electromechanical coupling provided by the piezoelectric actuators/sensors. Nevertheless, few studies focus on the optimization of this coupling for given structure and piezoelectric material. In particular, it has been shown that piezoelectric actuators using their thickness-shear mode can be more effective than surface-mounted extension piezoelectric actuators for both active (Trindade, Benjeddou and Ohayon, 1999; Raja, Prathap and Sinha, 2002; Baillargeon and Vel, 2005) and passive (Benjeddou and Ranger-Vieillard, 2004; Benjeddou, 2006; Trindade and Maio, 2006) vibration damping. One of the reasons for that is the thickness-shear electromechanical coupling coefficient k_{15} is normally twice the value of the extension one k_{31}. The thickness-shear mode, originally proposed by Sun and Zhang (1995), can be obtained using longitudinally-poled piezoelectric patches that couple through-thickness electric fields/displacements and shear strains/stresses.

This work presents the modeling of sandwich structures with extension and thickness-shear piezoelectric sensors/actuators connected to APPN. The model is based on a stress-voltage electromechanical model for the piezoelectric materials fully coupled to the APPN active-passive circuit. To this end, the APPN circuit equations are also included in the variational

formulation. Hence, conservation of charge and full electromechanical coupling are guaranteed. The formulation results in a coupled finite element model with mechanical (displacements) and electrical (electrodes charges) degrees of freedom. An analysis of the resulting equations of motion is performed to identify the damping mechanisms provided by an active-passive piezoelectric network.

2. THEORETICAL FORMULATION

Consider a sandwich beam made of piezoelectric layers and modeled using a classical sandwich theory. Surface layers are made of transversely poled piezoelectric materials, whereas the core layer is considered to be made of longitudinally poled piezoelectric materials. Electrodes fully cover the top and bottom skins of all layers so that only through-thickness electric field and displacement are considered. For simplicity, all layers are assumed to be made of orthotropic piezoelectric materials, perfectly bonded and in plane stress state. Bernoulli-Euler theory is retained for the sandwich beam surface layers, while the core is assumed to behave as a Timoshenko beam. The length, width and thickness of the beam are denoted by L, b and h, respectively. In addition, it is supposed that each piezoelectric actuator/sensor can be connected to an electric circuit composed of an inductance L_{cj}, a resistance R_{cj} and a voltage source φ_{cj} in series, with $j = 1,...,n$ where n is the number of piezoelectric transducer - circuit pairs.

2.1 Displacements and strains

The axial and transverse displacement fields of faces and core may be written in the following general form,

$$\begin{aligned} \bar{u}_i(x,y,z) &= u_i(x) + (z - z_i)\beta_i(x) \; ; \quad i = 1,2,3 \\ \bar{v}_i(x,y,z) &= 0 \\ \bar{w}_i(x,y,z) &= w(x) \end{aligned} \tag{1}$$

where u_i is the mid-plane axial displacement of the i-th layer ($i = 1$ for the top layer, $i = 2$ for the core layer and $i = 3$ for the bottom layer). β_i is the cross-section rotation angle and from Bernoulli-Euler assumptions $\beta_1 = \beta_3 = -w'$, where w' states for $\partial w/\partial x$. z_i states for the position of the i-th layer mid-plane in the global transversal z direction. Using the displacement continuity conditions between layers, the displacement fields may be written in terms of only three main variables, u_1, u_3 and w, so that u_2 and β_2 are written as

$$u_2 = \frac{u_1 + u_3}{2} + \frac{h_d}{4} w' \quad \text{and} \quad \beta_2 = \frac{u_1 - u_3}{h_2} + \frac{h_m}{h_2} w' \tag{2}$$

with h_m and h_d being the mean and difference of the surface layers thicknesses, h_1 and h_3,

$$h_m = \frac{h_1 + h_3}{2} \text{ and } h_d = h_1 - h_3 \tag{3}$$

The usual strain-displacement relations for each layer yield the following axial and shear strains for the i-th layer

$$\varepsilon_{1i} = \frac{\partial \bar{u}_i}{\partial x} = \varepsilon_i^m + (z - z_i)\varepsilon_i^f \quad \text{and} \quad \varepsilon_{5i} = \frac{\partial \bar{u}_i}{\partial z} + \frac{\partial \bar{w}_i}{\partial x} = \varepsilon_i^c \tag{4}$$

while the remaining strains ε_{2i}, ε_{3i}, ε_{4i} and ε_{6i} vanish. The membrane, bending and shear generalized strains, ε_i^m, ε_i^f and ε_i^c, can be written as

$$\varepsilon_k^m = u_k' \; ; \; \varepsilon_k^f = -w'' \; ; \; \varepsilon_k^c = 0 \; ; \; \text{for surface layers } (k = 1,3) \tag{5}$$

$$\varepsilon_2^m = \frac{u_1' + u_3'}{2} + \frac{h_d}{4} w'' \; ; \; \varepsilon_2^f = \frac{u_1' - u_3'}{h_2} + \frac{h_m}{h_2} w'' \; ; \; \varepsilon_2^c = \frac{u_1 - u_3}{h_2} + \left(\frac{h_m}{h_2} + 1 \right) w' \tag{6}$$

2.2 Piezoelectric constitutive equations

Linear orthotropic piezoelectric materials with material symmetry axes parallel to the beam ones are considered here, where c_{ij}^D, h_{lj} and β_l^ε $(i, j = 1,...,6; l = 1,2,3)$ denote their elastic (for constant electric displacement), piezoelectric and dielectric (for constant strain) material constants, respectively. For both extension and shear mode piezoelectric layers, only transverse electric field and displacements are considered ($D_1 = D_2 = 0$) since the layers have electrodes on top

and bottom skins. However, faces and core layers are treated separately, since they have different poling directions. An additional assumption of plane stress state ($\sigma_3 = 0$) allows to write the following reduced constitutive equations for the faces and the core

$$\begin{Bmatrix} \sigma_{1k} \\ E_{3k} \end{Bmatrix} = \begin{bmatrix} \bar{c}_{11}^{Dk} & -\bar{h}_{31}^{k} \\ -\bar{h}_{31}^{k} & \bar{\beta}_{33}^{\varepsilon k} \end{bmatrix} \begin{Bmatrix} \varepsilon_{1k} \\ D_{3k} \end{Bmatrix} \tag{7}$$

$$\begin{Bmatrix} \sigma_1 \\ \sigma_5 \\ E_3 \end{Bmatrix} = \begin{bmatrix} \bar{c}_{33}^{D2} & 0 & 0 \\ 0 & c_{55}^{D2} & -h_{15}^{2} \\ 0 & -h_{15}^{2} & \beta_{11}^{\varepsilon 2} \end{bmatrix} \begin{Bmatrix} \varepsilon_{12} \\ \varepsilon_{52} \\ D_{32} \end{Bmatrix} \tag{8}$$

where,

$$\bar{c}_{11}^{Dk} = c_{11}^{Dk} - c_{13}^{Dk}\frac{c_{13}^{Dk}}{c_{33}^{Dk}} \; ; \; \bar{h}_{31}^{k} = h_{31}^{k} - h_{33}^{k}\frac{c_{13}^{Dk}}{c_{33}^{Dk}} \; ; \; \bar{\beta}_{33}^{\varepsilon k} = \beta_{33}^{\varepsilon k} + \frac{{h_{33}^{k}}^2}{c_{33}^{Dk}} \; ; \; \bar{c}_{33}^{D2} = c_{33}^{D2} - c_{13}^{D2}\frac{c_{13}^{D2}}{c_{11}^{D2}}$$

2.3 Variational formulation

The equation of motions can be written using the variational principle of d'Alembert extended to piezoelectric media

$$\delta T - \delta H + \delta W = 0 \tag{9}$$

where δT, δH and δW are the virtual work done by inertial, internal and external forces. These are composed of contributions from the three piezoelectric layers and the n electric circuits connected to the structure, such that

$$\delta T = \sum_{i=1}^{3} \delta T_{mi} + \sum_{j=1}^{n} \delta T_{cj} \; ; \; \delta H = \sum_{i=1}^{3} (\delta H_{mi} + \delta H_{mei} + \delta H_{ei}) \; ; \; \delta W = \sum_{i=1}^{3} W_{mi} + \sum_{j=1}^{n} (\delta W_{rj} + \delta W_{ej}) \tag{10}$$

Each of these virtual work contributions are detailed in the following subsections.

2.3.1 Virtual work done by inertial forces

The virtual work done by inertial forces for the i-th layer of the sandwich beam can be written as

$$\delta T_{mi} = -\int_V (\delta \bar{u}_i \rho_i \ddot{\bar{u}}_i + \delta \bar{w}_i \rho_i \ddot{\bar{w}}_i) \mathrm{d}V \tag{11}$$

where ρ_i is the mass density of the i-th layer and the dot stands for time derivation. Using the displacements fields defined in (1), this expression can be rewritten as

$$\delta T_{mi} = -\int_V \left[\rho_i (\delta u_i \ddot{u}_i + \delta w \ddot{w}) + \rho_i (z - z_i)(\delta u_i \ddot{\beta}_i + \delta \beta_i \ddot{u}_i) + \rho_i (z - z_i)^2 \delta \beta_i \ddot{\beta}_i \right] \mathrm{d}V \tag{12}$$

Then, supposing that all layers are symmetric with respect to their neutral lines, $z = z_i$, and integrating in cross-section area leads to

$$\delta T_{mi} = -\int_0^L \left[\rho_i A_i (\delta u_i \ddot{u}_i + \delta w \ddot{w}) + \rho_i I_i \delta \beta_i \ddot{\beta}_i \right] \mathrm{d}x \tag{13}$$

where A_i and I_i are the area and second moment of area of the cross-section, respectively.

2.3.2 Virtual work done by internal (electromechanical) forces

To obtain the virtual work done by internal electromechanical forces, the electromechanical entropy of a piezoelectric layer is written as

$$H(\varepsilon,\mathbf{D}) = \frac{1}{2}\varepsilon^{\mathrm{t}}\mathbf{c}^{D}\varepsilon - \varepsilon^{\mathrm{t}}\mathbf{h}\mathbf{D} + \frac{1}{2}\mathbf{D}^{\mathrm{t}}\beta^{\varepsilon}\mathbf{D} \tag{14}$$

where ε and $\mathbf{D}$ are the mechanical strains and electric displacements vectors, and $\mathbf{c}^{D}$, $\mathbf{h}$ and β^{ε} are the elastic, piezoelectric and dielectric constants matrices. The virtual work done by internal electromechanical forces can be written from the virtual variation of the entropy H and will be composed of mechanical δH_m, electromechanical (piezoelectric) δH_{me}, and dielectric δH_e contributions. In what follows, these are detailed for the faces $k = 1,3$ and core $i = 2$ layer. Hence, for the faces,

$$\delta H_{mk} = \int_V \delta\varepsilon_{1k}\bar{c}_{11}^{Dk}\varepsilon_{1k}\mathrm{d}V \tag{15}$$

Using the normal strain expression for the faces, from (4), leads to

$$\delta H_{mk} = \int_V \left[\delta\varepsilon_k^m\bar{c}_{11}^{Dk}\varepsilon_k^m + (z-z_k)(\delta\varepsilon_k^m\bar{c}_{11}^{Dk}\varepsilon_k^f + \delta\varepsilon_k^f\bar{c}_{11}^{Dk}\varepsilon_k^m) + (z-z_k)^2\delta\varepsilon_k^f\bar{c}_{11}^{Dk}\varepsilon_k^f\right]\mathrm{d}V \tag{16}$$

which, supposing symmetric layers and integrating in the cross-section, can be reduced to

$$\delta H_{mk} = \int_0^L \left(\delta\varepsilon_k^m\bar{c}_{11}^{Dk}A_k\varepsilon_k^m + \delta\varepsilon_k^f\bar{c}_{11}^{Dk}I_k\varepsilon_k^f\right)\mathrm{d}x \tag{17}$$

For the core layer ($i = 2$), both normal and shear strains contribute to the virtual work of mechanical internal forces, such that

$$\delta H_{m2} = \int_V \left(\delta\varepsilon_{12}\bar{c}_{33}^{D2}\varepsilon_{12} + \delta\varepsilon_{52}c_{55}^{D2}\varepsilon_{52}\right)\mathrm{d}V \tag{18}$$

Using the normal and shear strain expression for the core, from (4), and, supposing a symmetric core layer and integrating in the cross-section, leads to

$$\delta H_{m2} = \int_0^L \left(\delta\varepsilon_2^m\bar{c}_{33}^{D2}A_2\varepsilon_2^m + \delta\varepsilon_2^f\bar{c}_{33}^{D2}I_2\varepsilon_2^f + \delta\varepsilon_2^c k_2 c_{55}^{D2}A_2\varepsilon_2^c\right)\mathrm{d}x \tag{19}$$

where k_2 is the shear correction factor.

The piezoelectric contributions to the virtual work of internal forces can be written, for the faces,

$$\delta H_{mek} = -\int_V \left(\delta\varepsilon_{1k}\bar{h}_{31}^k D_{3k} + \delta D_{3k}\bar{h}_{31}^k\varepsilon_{1k}\right)\mathrm{d}V \tag{20}$$

and, for the core,

$$\delta H_{me2} = -\int_V \left(\delta\varepsilon_{52}h_{15}D_{32} + \delta D_{32}h_{15}\varepsilon_{52}\right)\mathrm{d}V \tag{21}$$

Notice that the piezoelectric effect couples the transversal electric displacement D_{3i} with normal strain ε_{1k}, for the faces, and with shear strain ε_{52}, for the core. Supposing symmetric layers and integrating in the cross-section, these can be written as

$$\delta H_{mek} = -\int_0^L \left(\delta\varepsilon_k^m\bar{h}_{31}^k A_k D_{3k} + \delta D_{3k}\bar{h}_{31}^k A_k\varepsilon_k^m\right)\mathrm{d}x \tag{22}$$

$$\delta H_{me2} = -\int_0^L \left(\delta\varepsilon_2^c h_{15}A_2 D_{32} + \delta D_{32}h_{15}A_2\varepsilon_2^c\right)\mathrm{d}x \tag{23}$$

The dielectric contribution to the virtual work of internal forces can be written as

$$\delta H_{ek} = \int_V \left(\delta D_{3k} \bar{\beta}_{33}^{\varepsilon k} D_{3k} \right) \mathrm{d}V \text{ and } \delta H_{e2} = \int_V \left(\delta D_{32} \beta_{11}^{\varepsilon 2} D_{32} \right) \mathrm{d}V \tag{24}$$

which, through integration in the cross-section, read

$$\delta H_{ek} = \int_0^L \left(\delta D_{3k} \bar{\beta}_{33}^{\varepsilon k} A_k D_{3k} \right) \mathrm{d}x \text{ and } \delta H_{e2} = \int_0^L \left(\delta D_{32} \beta_{11}^{\varepsilon 2} A_2 D_{32} \right) \mathrm{d}x \tag{25}$$

2.3.3 Virtual work done by external mechanical forces

Each layer of the sandwich beam is also supposed to be subjected to axial and transversal body forces, applied at their neutral lines. The virtual work due to these forces can be written as

$$\delta W_{mi} = \int_V \left(\delta u_i f_{xi} + \delta w f_{yi} \right) \mathrm{d}V \tag{26}$$

Integration in the cross-section leads to

$$\delta W_{mi} = \int_0^L \left(\delta u_i f_{xi} A_i + \delta w f_{yi} A_i \right) \mathrm{d}x \tag{27}$$

2.3.4 Virtual work done by electric circuit components

The virtual work done by the inductances, δT_{cj}, resistances, δW_{rj}, and voltage sources, δW_{ej}, of the j-th electric circuit can be written as

$$\delta T_{cj} = -\delta q_{cj} L_{cj} \ddot{q}_{cj} \; ; \; \delta W_{rj} = -\delta q_{cj} R_{cj} \dot{q}_{cj} \; ; \; \delta W_{ej} = \delta q_{cj} \varphi_{cj} \tag{28}$$

where L_{cj}, R_{cj} and φ_{cj} are the inductance, resistance and applied voltage connected in series for the j-th electric circuit. q_{cj} is the electric charge entering the j-th electric circuit.

3. FINITE ELEMENT FORMULATION

Using the virtual work expressions presented previously, a finite element model for the piezoelectric sandwich beam is developed. Lagrange linear shape functions are assumed for the axial displacements, u_1 and u_3, and electric displacements in each layer, D_{31}, D_{32} and D_{33}. For the transverse deflection w, Hermite cubic shape functions are assumed.

3.1 Discretization of generalized displacements and strains

The elementary mechanical degrees of freedom (dof) column vector u_n is defined as

$$\mathbf{u}_n = \begin{bmatrix} u_1^1 & u_3^1 & w^1 & w'^1 & u_1^2 & u_3^2 & w^2 & w'^2 \end{bmatrix}^{\mathrm{t}} \tag{29}$$

The axial displacements of each layer can be written in terms of the elementary dofs as

$$u_i = \mathbf{N}_{xi} \mathbf{u}_n \tag{30}$$

where

$$\begin{aligned} \mathbf{N}_{x1} &= \begin{bmatrix} N_1 & 0 & 0 & 0 & N_2 & 0 & 0 & 0 \end{bmatrix} \\ \mathbf{N}_{x2} &= \begin{bmatrix} \frac{N_1}{2} & \frac{N_1}{2} & \frac{h_d}{4} N_3' & \frac{h_d}{4} N_4' & \frac{N_2}{2} & \frac{N_2}{2} & \frac{h_d}{4} N_5' & \frac{h_d}{4} N_6' \end{bmatrix} \\ \mathbf{N}_{x3} &= \begin{bmatrix} 0 & N_1 & 0 & 0 & 0 & N_2 & 0 & 0 \end{bmatrix} \end{aligned} \tag{31}$$

and

$$N_1 = 1 - \frac{x}{L} \; ; \; N_2 = \frac{x}{L} ; N_3 = 1 - \frac{3x^2}{L^2} + \frac{2x^3}{L^3} \; ; \; N_4 = x \left(1 - \frac{x}{L} \right)^2 \; ; \; N_5 = \frac{x^2}{L^2} \left(3 - \frac{2x}{L} \right) \; ; \; N_6 = \frac{x^2}{L} \left(\frac{x}{L} - 1 \right)$$

The transverse displacement w is written as

$$w = \mathbf{N}_z \mathbf{u}_n \tag{32}$$

where

$$\mathbf{N}_z = \begin{bmatrix} 0 & 0 & N_3 & N_4 & 0 & 0 & N_5 & N_6 \end{bmatrix} \tag{33}$$

The cross-section rotations β_i are written as

$$\beta_i = \mathbf{N}_{ri} \mathbf{u}_n \tag{34}$$

where

$$\begin{aligned} \mathbf{N}_{r1} &= \begin{bmatrix} 0 & 0 & -N_3' & -N_4' & 0 & 0 & -N_5' & -N_6' \end{bmatrix} \\ \mathbf{N}_{r2} &= \begin{bmatrix} \frac{N_1}{h_2} & \frac{-N_1}{h_2} & \frac{h_m N_3'}{h_2} & \frac{h_m N_4'}{h_2} & \frac{N_2}{h_2} & \frac{-N_2}{h_2} & \frac{h_m N_5'}{h_2} & \frac{h_m N_6'}{h_2} \end{bmatrix} \\ \mathbf{N}_{r3} &= \begin{bmatrix} 0 & 0 & -N_3' & -N_4' & 0 & 0 & -N_5' & -N_6' \end{bmatrix} \end{aligned} \tag{35}$$

According to the expressions (5) and (6) for the generalized strains, ε_i^m, ε_i^f, and ε_i^c, they can be written in terms of the elementary dofs as

$$\varepsilon_i^m = \mathbf{B}_{mi} \mathbf{u}_n \; ; \; \varepsilon_i^f = \mathbf{B}_{fi} \mathbf{u}_n \; ; \; \varepsilon_2^c = \mathbf{B}_{c2} \mathbf{u}_n \tag{36}$$

The membrane, bending and shear strain operators $\mathbf{B}_{mi}$, $\mathbf{B}_{fi}$ and $\mathbf{B}_{c2}$ are defined as

$$\begin{aligned} \mathbf{B}_{m1} &= \begin{bmatrix} N_1' & 0 & 0 & 0 & N_2' & 0 & 0 & 0 \end{bmatrix} \\ \mathbf{B}_{m2} &= \begin{bmatrix} \frac{N_1'}{2} & \frac{N_1'}{2} & \frac{h_d N_3''}{4} & \frac{h_d N_4''}{4} & \frac{N_2'}{2} & \frac{N_2'}{2} & \frac{h_d N_5''}{4} & \frac{h_d N_6''}{4} \end{bmatrix} \\ \mathbf{B}_{m3} &= \begin{bmatrix} 0 & N_1' & 0 & 0 & 0 & N_2' & 0 & 0 \end{bmatrix} \end{aligned} \tag{37}$$

$$\begin{aligned} \mathbf{B}_{f1} &= \begin{bmatrix} 0 & 0 & -N_3'' & -N_4'' & 0 & 0 & -N_5'' & -N_6'' \end{bmatrix} \\ \mathbf{B}_{f2} &= \begin{bmatrix} \frac{N_1'}{h_2} & \frac{-N_1'}{h_2} & \frac{h_m N_3''}{h_2} & \frac{h_m N_4''}{h_2} & \frac{N_2'}{h_2} & \frac{-N_2'}{h_2} & \frac{h_m N_5''}{h_2} & \frac{h_m N_6''}{h_2} \end{bmatrix} \\ \mathbf{B}_{f3} &= \begin{bmatrix} 0 & 0 & -N_3'' & -N_4'' & 0 & 0 & -N_5'' & -N_6'' \end{bmatrix} \end{aligned} \tag{38}$$

$$\mathbf{B}_{c2} = \begin{bmatrix} \frac{N_1}{h_2} & \frac{-N_1}{h_2} & \frac{h_m+h_2}{h_2} N_3'' & \frac{h_m+h_2}{h_2} N_4'' & \frac{N_2}{h_2} & \frac{-N_2}{h_2} & \frac{h_m+h_2}{h_2} N_5'' & \frac{h_m+h_2}{h_2} N_6'' \end{bmatrix} \tag{39}$$

3.2 Discretization of electric displacements

The elementary electric dofs column vector D_n is defined as

$$\mathbf{D}_n = \begin{bmatrix} D_{31}^1 & D_{32}^1 & D_{33}^1 & D_{31}^2 & D_{32}^2 & D_{33}^2 \end{bmatrix}^{\mathrm{t}} \tag{40}$$

Then, the electric displacement in the piezoelectric layers can be written in terms of the elementary dofs

$$D_{3i} = \mathbf{N}_{Di} \mathbf{D}_n \tag{41}$$

where,

$$\begin{aligned} \mathbf{N}_{D1} &= \begin{bmatrix} N_1 & 0 & 0 & N_2 & 0 & 0 \end{bmatrix} \\ \mathbf{N}_{D2} &= \begin{bmatrix} 0 & N_1 & 0 & 0 & N_2 & 0 \end{bmatrix} \\ \mathbf{N}_{D3} &= \begin{bmatrix} 0 & 0 & N_1 & 0 & 0 & N_2 \end{bmatrix} \end{aligned} \tag{42}$$

3.3 Discretization of virtual work expressions

In this subsection, the discretized mechanical displacements and strains and electric displacements are substituted into the virtual work expressions to obtain their discretized versions.

Hence, from (13) and (30), (32) and (34), the virtual work of inertial forces can be rewritten as

$$\delta T_{mi} = -\delta \mathbf{u}_n^{\mathrm{t}} \mathbf{M}_i \ddot{\mathbf{u}}_n \tag{43}$$

where $\mathbf{M}_i$ is mass matrix of the i-th layer defined as

$$\mathbf{M}_i = \int_0^L \left[\rho_i A_i (\mathbf{N}_{xi}^{\mathrm{t}} \mathbf{N}_{xi} + \mathbf{N}_{zi}^{\mathrm{t}} \mathbf{N}_{zi}) + \rho_i I_i \mathbf{N}_{ri}^{\mathrm{t}} \mathbf{N}_{ri} \right] \mathrm{d}x \tag{44}$$

The mechanical contribution to the virtual work of the internal electromechanical forces can be discretized from (17), for the faces, and (19), for the core, combined to the discretization of the generalized strains (36), such as

$$\delta H_{mi} = \delta \mathbf{u}_n^{\mathrm{t}} \mathbf{K}_{mi} \mathbf{u}_n \tag{45}$$

where, for the faces ($k = 1, 3$),

$$\mathbf{K}_{mk} = \int_0^L \left(\mathbf{B}_{mk}^{\mathrm{t}} \bar{c}_{11}^{Dk} A_k \mathbf{B}_{mk} + \mathbf{B}_{fk}^{\mathrm{t}} \bar{c}_{11}^{Dk} I_k \mathbf{B}_{fk} \right) \mathrm{d}x \tag{46}$$

and, for the core layer,

$$\mathbf{K}_{m2} = \int_0^L \left(\mathbf{B}_{m2}^{\mathrm{t}} \bar{c}_{33}^{D2} A_2 \mathbf{B}_{m2} + \mathbf{B}_{f2}^{\mathrm{t}} \bar{c}_{33}^{D2} I_2 \mathbf{B}_{f2} + \mathbf{B}_{c2}^{\mathrm{t}} k_2 c_{55}^{D2} A_2 \mathbf{B}_{c2} \right) \mathrm{d}x \tag{47}$$

From (22), for the faces, and (23), for the core, and the discretized expression for the the generalized strains (36) and electric displacements (41), the piezoelectric contributions to the virtual work of internal electromechanical forces can be written as

$$\delta H_{mei} = -\delta \mathbf{u}_n^{\mathrm{t}} \mathbf{K}_{mei} \mathbf{D}_n - \delta \mathbf{D}_n^{\mathrm{t}} \mathbf{K}_{mei}^{\mathrm{t}} \mathbf{u}_n \tag{48}$$

where $\mathbf{K}_{mei}$ states for the electromechanical (piezoelectric) stiffness matrices, which are defined as, for the faces,

$$\mathbf{K}_{mek} = \int_0^L \left(\mathbf{B}_{mk}^{\mathrm{t}} \bar{h}_{31}^{k} A_k \mathbf{N}_{Dk} \right) \mathrm{d}x \tag{49}$$

and, for the core layer,

$$\mathbf{K}_{me2} = \int_0^L \left(\mathbf{B}_{c2}^{\mathrm{t}} h_{15} A_2 \mathbf{N}_{D2} \right) \mathrm{d}x \tag{50}$$

The dielectric contributions to the virtual work of internal forces may also be discretized from (25) and (41) such as

$$\delta H_{ei} = \delta \mathbf{D}_n^{\mathrm{t}} \mathbf{K}_{ei} \mathbf{D}_n \tag{51}$$

where $\mathbf{K}_e i$ are the dielectric stiffness matrices written as, for the faces,

$$\mathbf{K}_{ek} = \int_0^L \left(\mathbf{N}_{Dk}^{\mathrm{t}} \bar{\beta}_{33}^{\varepsilon k} A_k \mathbf{N}_{Dk} \right) \mathrm{d}x \tag{52}$$

and, for the core layer,

$$\mathbf{K}_{e2} = \int_0^L \left(\mathbf{N}_{D2}^{\mathrm{t}} \beta_{11}^{\varepsilon 2} A_2 \mathbf{N}_{D2} \right) \mathrm{d}x \tag{53}$$

The virtual work done by external mechanical forces can be discretized replacing (30) and (32) in (27), such that

$$\delta W_{mi} = \delta \mathbf{u}_n^{\mathrm{t}} \mathbf{F}_i \tag{54}$$

where $\mathbf{F}_i$ states for the vector of applied mechanical forces for the i-th layer,

$$\mathbf{F}_i = \int_0^L \left(\mathbf{N}_{xi}^{\mathrm{t}} f_{xi} A_i + \mathbf{N}_z^{\mathrm{t}} f_{yi} A_i \right) \mathrm{d}x \tag{55}$$

3.4 Equations of motion

The discretized virtual work expressions can now be replaced in the principle of d'Alembert (9) leading to

$$\delta \mathbf{u}_n^{\mathrm{t}} \left(\mathbf{M}^e \ddot{\mathbf{u}}_n + \mathbf{K}_m^e \mathbf{u}_n - \mathbf{K}_{me}^e \mathbf{D}_n - \mathbf{F}^e \right) + \delta \mathbf{D}_n^{\mathrm{t}} \left(-\mathbf{K}_{me}^{e\,\mathrm{t}} \mathbf{u}_n + \mathbf{K}_e^e \mathbf{D}_n \right) + \delta \mathbf{q}_c^{\mathrm{t}} \left(-\mathbf{L}_c \ddot{\mathbf{q}}_c - \mathbf{R}_c \dot{\mathbf{q}}_c + \varphi_c \right) = 0 \tag{56}$$

where the elementary mass and stiffness matrices and mechanical forces vector are

$$\mathbf{M}^e = \sum_{i=1}^{3} \mathbf{M}_i \; ; \; \mathbf{K}_{me}^e = \sum_{i=1}^{3} \mathbf{K}_{mei} \; ; \; \mathbf{K}_e^e = \sum_{i=1}^{3} \mathbf{K}_{ei} \; ; \; \mathbf{F}^e = \sum_{i=1}^{3} \mathbf{F}_i$$

Therefore, the following equations of motion can be written

$$\begin{bmatrix} \mathbf{M}^e & 0 & 0 \\ 0 & 0 & 0 \\ 0 & 0 & \mathbf{L}_c \end{bmatrix} \begin{Bmatrix} \ddot{\mathbf{u}}_n \\ \ddot{\mathbf{D}}_n \\ \ddot{\mathbf{q}}_c \end{Bmatrix} + \begin{bmatrix} 0 & 0 & 0 \\ 0 & 0 & 0 \\ 0 & 0 & \mathbf{R}_c \end{bmatrix} \begin{Bmatrix} \dot{\mathbf{u}}_n \\ \dot{\mathbf{D}}_n \\ \dot{\mathbf{q}}_c \end{Bmatrix} + \begin{bmatrix} \mathbf{K}_m^e & -\mathbf{K}_{me}^e & 0 \\ -\mathbf{K}_{me}^{e\,\mathrm{t}} & \mathbf{K}_e^e & 0 \\ 0 & 0 & 0 \end{bmatrix} \begin{Bmatrix} \mathbf{u}_n \\ \mathbf{D}_n \\ \mathbf{q}_c \end{Bmatrix} = \begin{Bmatrix} \mathbf{F}^e \\ 0 \\ \varphi_c \end{Bmatrix} \tag{57}$$

Assembling for all finite elements of the structure, the equations of motion can be expressed as

$$\begin{bmatrix} \mathbf{M} & 0 & 0 \\ 0 & 0 & 0 \\ 0 & 0 & \mathbf{L}_c \end{bmatrix} \begin{Bmatrix} \ddot{\mathbf{u}} \\ \ddot{\mathbf{D}} \\ \ddot{\mathbf{q}}_c \end{Bmatrix} + \begin{bmatrix} 0 & 0 & 0 \\ 0 & 0 & 0 \\ 0 & 0 & \mathbf{R}_c \end{bmatrix} \begin{Bmatrix} \dot{\mathbf{u}} \\ \dot{\mathbf{D}} \\ \dot{\mathbf{q}}_c \end{Bmatrix} + \begin{bmatrix} \mathbf{K}_m & -\mathbf{K}_{me} & 0 \\ -\mathbf{K}_{me}^{\mathrm{t}} & \mathbf{K}_e & 0 \\ 0 & 0 & 0 \end{bmatrix} \begin{Bmatrix} \mathbf{u} \\ \mathbf{D} \\ \mathbf{q}_c \end{Bmatrix} = \begin{Bmatrix} \mathbf{F} \\ 0 \\ \varphi_c \end{Bmatrix} \tag{58}$$

where $\mathbf{u}$ and $\mathbf{D}$ are the global mechanical and electric dofs and the mass and stiffness matrices and mechanical force vector were assembled for all finite elements.

To account for the electrodes fully covering the piezoelectric patches top and bottom skins, the electric displacements of selected nodes and layers are set to be equal. This dof assignment can be represented by the following expression

$$\mathbf{D} = \mathbf{L}_p \mathbf{D}_p \tag{59}$$

where $\mathbf{L}_p$ is a binary matrix and $\mathbf{D}_p$ is a vector of the electric displacement for one piezoelectric patch (constant throughout the electrode surface),

$$\mathbf{D}_p = \begin{bmatrix} D_{p1} & D_{p2} & \cdots & D_{pn} \end{bmatrix}^{\mathrm{t}} \tag{60}$$

Substituting (59) into (58), the equations of motion are reduced to

$$\begin{bmatrix} \mathbf{M} & 0 & 0 \\ 0 & 0 & 0 \\ 0 & 0 & \mathbf{L}_c \end{bmatrix} \begin{Bmatrix} \ddot{\mathbf{u}} \\ \ddot{\mathbf{D}}_p \\ \ddot{\mathbf{q}}_c \end{Bmatrix} + \begin{bmatrix} 0 & 0 & 0 \\ 0 & 0 & 0 \\ 0 & 0 & \mathbf{R}_c \end{bmatrix} \begin{Bmatrix} \dot{\mathbf{u}} \\ \dot{\mathbf{D}}_p \\ \dot{\mathbf{q}}_c \end{Bmatrix} + \begin{bmatrix} \mathbf{K}_m & -\bar{\mathbf{K}}_{me} & 0 \\ -\bar{\mathbf{K}}_{me}^{\mathrm{t}} & \bar{\mathbf{K}}_e & 0 \\ 0 & 0 & 0 \end{bmatrix} \begin{Bmatrix} \mathbf{u} \\ \mathbf{D}_p \\ \mathbf{q}_c \end{Bmatrix} = \begin{Bmatrix} \mathbf{F} \\ 0 \\ \varphi_c \end{Bmatrix} \tag{61}$$

where

$$\bar{\mathbf{K}}_{me} = \mathbf{K}_{me} \mathbf{L}_p \; ; \; \bar{\mathbf{K}}_e = \mathbf{L}_p^{\mathrm{t}} \mathbf{K}_e \mathbf{L}_p \tag{62}$$

4. CONNECTING PIEZOELECTRIC PATCHES TO ELECTRIC CIRCUITS

To account for the connection between piezoelectric patches and electric circuits, it is supposed that electric charges entering a given electric circuit are equal to electric charges of a given piezoelectric patch. This relation can be written as

$$\mathbf{q}_c = \mathbf{L}_q \mathbf{q}_p \tag{63}$$

where $\mathbf{L}_q$ is an binary assignment matrix. Since, due to equipotentiality condition in the electrodes, the electric displacement is constant throughout the electrode surface, the electric charges for a given piezoelectric patch is obtained by multiplying the electric displacement by the electrode area. Thus, a diagonal matrix $\mathbf{A}_q$ which elements are the electrodes areas of each piezoelectric patch is defined. Then, the vector of electric charges is written as

$$\mathbf{q}_p = \mathbf{A}_q \mathbf{D}_p \tag{64}$$

Hence, the electric charges entering the n electric circuits can be written in terms of the piezoelectric patches electric displacements as

$$\mathbf{q}_c = \mathbf{B}_q \mathbf{D}_p \; ; \quad \mathbf{B}_q = \mathbf{L}_q \mathbf{A}_q \tag{65}$$

Therefore, the coupled equations of motion can be written as

$$\begin{bmatrix} \mathbf{M} & 0 \\ 0 & \mathbf{M}_q \end{bmatrix} \begin{Bmatrix} \ddot{\mathbf{u}} \\ \ddot{\mathbf{D}}_p \end{Bmatrix} + \begin{bmatrix} 0 & 0 \\ 0 & \mathbf{C}_q \end{bmatrix} \begin{Bmatrix} \dot{\mathbf{u}} \\ \dot{\mathbf{D}}_p \end{Bmatrix} + \begin{bmatrix} \mathbf{K}_m & -\bar{\mathbf{K}}_{me} \\ -\bar{\mathbf{K}}_{me}^{\mathrm{t}} & \bar{\mathbf{K}}_e \end{bmatrix} \begin{Bmatrix} \mathbf{u} \\ \mathbf{D}_p \end{Bmatrix} = \begin{Bmatrix} \mathbf{F} \\ \mathbf{F}_q \end{Bmatrix} \tag{66}$$

where

$$\mathbf{M}_q = \mathbf{B}_q^{\mathrm{t}} \mathbf{L}_c \mathbf{B}_q \; ; \; \mathbf{C}_q = \mathbf{B}_q^{\mathrm{t}} \mathbf{R}_c \mathbf{B}_q \; ; \; \mathbf{F}_q = \mathbf{B}_q^{\mathrm{t}} \varphi_c \tag{67}$$

5. RESPONSE TO ELECTRIC HARMONIC EXCITATION

In this section, a harmonic analysis is performed to obtain a preliminary evaluation of the effects caused by the electric circuit components on the structure. For that, an electric harmonic excitation is considered for a simple case with only one piezoelectric patch connected to a RLV circuit (resistance - inductance - voltage source) and without applied mechanical forces, such that

$$\varphi_c = \tilde{\varphi}_c e^{i\omega t} \; ; \; \mathbf{u} = \tilde{\mathbf{u}} e^{i\omega t} \; ; \; \mathbf{D}_p = \tilde{\mathbf{D}}_p e^{i\omega t} \tag{68}$$

Therefore, the equations of motion (66) can be rewritten as

$$\begin{aligned} (-\omega^2 \mathbf{M} + \mathbf{K}_m)\tilde{\mathbf{u}} - \bar{\mathbf{K}}_{me}\tilde{\mathbf{D}}_p &= 0 \\ -\bar{\mathbf{K}}_{me}^{\mathrm{t}}\tilde{\mathbf{u}} + (-\omega^2 \mathbf{M}_q + i\omega \mathbf{C}_q + \bar{\mathbf{K}}_e)\tilde{\mathbf{D}}_p &= \mathbf{B}_q^{\mathrm{t}} \tilde{\varphi}_c \end{aligned} \tag{69}$$

Solving the second equation for $\tilde{\mathbf{D}}_p$ and replacing in the first equation, leads to

$$\left\{ -\omega^2 \mathbf{M} + \left[\mathbf{K}_m - \bar{\mathbf{K}}_{me}(-\omega^2 \mathbf{M}_q + i\omega \mathbf{C}_q + \bar{\mathbf{K}}_e)^{-1} \bar{\mathbf{K}}_{me}^{\mathrm{t}} \right] \right\} \tilde{\mathbf{u}} = \bar{\mathbf{K}}_{me}(-\omega^2 \mathbf{M}_q + i\omega \mathbf{C}_q + \bar{\mathbf{K}}_e)^{-1} \mathbf{B}_q^{\mathrm{t}} \tilde{\varphi}_c \tag{70}$$

Considering the measurement of the displacement in a selected point of the structure such that

$$\tilde{y} = \mathbf{c}_p \tilde{\mathbf{u}} \tag{71}$$

where $\tilde{\mathbf{y}}$ is a scalar and $\mathbf{c}_p$ is an output distribution vector. Then, the frequency response function of $\tilde{y}$ subjected to the applied voltage $\tilde{\varphi}_c$ can be obtained from

$$\tilde{y} = G(\omega)\tilde{\varphi}_c \tag{72}$$

where

$$G(\omega) = \left\{-\omega^2\mathbf{M} + \left[\mathbf{K}_m - \bar{\mathbf{K}}_{me}(-\omega^2\mathbf{M}_q + i\omega\mathbf{C}_q + \bar{\mathbf{K}}_e)^{-1}\bar{\mathbf{K}}_{me}^{\mathrm{t}}\right]\right\}^{-1}\bar{\mathbf{K}}_{me}(-\omega^2\mathbf{M}_q + i\omega\mathbf{C}_q + \bar{\mathbf{K}}_e)^{-1}\mathbf{B}_q^{\mathrm{t}} \tag{73}$$

From the expression for $G(\omega)$, one may notice that the resistance and inductance components of the electric circuit have two effects. First, they lead to a passive modification on the structure stiffness. This can be observed in the term between braces of (73). In particular, it should be noticed that for a circuit without resistance and inductance, that is $\mathbf{M}_q = \mathbf{C}_q = 0$, the stiffness modification reduces to the stiffness corresponding to short-circuit condition, while the open-circuit condition can be obtained by setting $\mathbf{C}_q \to \infty$, that is a very large resistance. On the other hand, for the general case, the presence of a resistance in the electric circuit leads to a complex valued stiffness matrix which can be interpreted as a hysteretic damping matrix. The relative importance of the imaginary part of the stiffness matrix is clearly dependent on the electromechanical coupling, via piezoelectric $\bar{\mathbf{K}}_{me}$ and dielectric $\bar{\mathbf{K}}_e$ matrices, and the resistance and inductance values, via $\mathbf{M}_q$ and $\mathbf{C}_q$.

The second effect of the resistance and inductance components on the frequency response function $G(\omega)$ is that in addition to the structure resonances, the passive electric circuit components (RL) also affects the electric excitation amplitude, via the term $\bar{\mathbf{K}}_{me}(-\omega^2\mathbf{M}_q + i\omega\mathbf{C}_q + \bar{\mathbf{K}}_e)^{-1}\mathbf{B}_q^{\mathrm{t}}$. This means that the RL components can amplify the excitation amplitude for a given frequency range. Hence, with properly tuned RL components it could be possible to amplify an active control action applied by the voltage source. This analysis is in accordance with the observations of Tsai and Wang (1999). However, it should be noticed that the tuning of the active control amplification and the passive RL damping are not independent and, thus, should be optimized simultaneously.

6. NUMERICAL RESULTS

This section presents some numerical results with shear and extension piezoceramics connected to APPN. In particular, the passive damping capability and the control authority of both mechanisms are evaluated. To this end, the configurations depicted in Figure 1 are considered. The extension and shear piezoceramic sensors/actuators are made of PZT-5H material whose properties are: $\bar{c}_{11}^D = 97.767$ GPa, $\bar{c}_{33}^D = 119.71$ GPa, $c_{55}^D = 42.217$ GPa, $\rho = 7500$ kg m^{-3}, piezoelectric coupling constants $\bar{h}_{31} = -1.3520\ 10^9$ N C^{-1} and $h_{15} = 1.1288\ 10^9$ N C^{-1}, and dielectric constants $\bar{\beta}_{33}^{\varepsilon} = 99.740\ 10^6$ m F^{-1} and $\beta_{11}^{\varepsilon} = 66.267\ 10^6$ m F^{-1}. For the Aluminium beam, material properties are: Young's modulus 70.3 GPa and density 2710 kg m^{-3} and, for the foam, Young's modulus 35.3 MPa, shear modulus 12.7 MPa and density 32 kg m^{-3}. An initial viscous damping of 0.5% was considered.

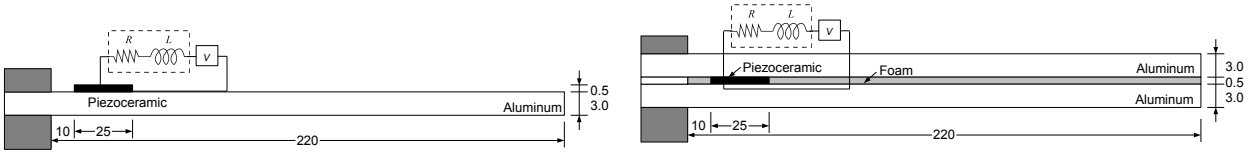

Figure 1. Representation of cantilever beam with extension and shear piezoceramic sensors/actuators.

The frequency responses of both configurations were analyzed in order to evaluate first the passive damping capability of the APPN circuit and then the effect of the APPN circuit on the control authority of the piezoceramic actuator. This was done by evaluating the frequency response of the beam tip velocity when excited by a transversal mechanical force applied at the beam tip and by a control voltage applied to the piezoceramic actuators. The optimal resistance and inductance values for the resistive and resonant cases were evaluated using the formulas proposed by Tsai and Wang (1999) and Trindade and Maio (2006). Figure 2 presents the frequency responses for the extension configuration. In Figure 2a, it is possible to observe that proper tuning of the resistive and resonant circuits can yield considerable amplitude reduction near the first resonance frequency. On the other hand, Figure 2b shows that the control authority near the first resonance can be increased by the RL circuit, while it is decreased for higher frequencies.

The same analysis was performed for the shear configuration. Figure 3a shows the frequency response near the first resonance. It can be observed that, as for the extension configuration, the vibration amplitude can also be reduced by proper tuning of resistance and inductance values. Notice however that, in this case, the control authority near the first resonance can be significantly increased by the RL circuit, while it is decreased for higher frequencies (Figure 3b).

7. CONCLUSIONS

This work has presented the modeling of sandwich structures with extension and thickness-shear piezoelectric sensors/actuators connected to APPN. The proposed model is based on a stress-voltage electromechanical model for the piezoelectric materials fully coupled to the APPN active-passive circuit and results in a coupled finite element model with mechanical (displacements) and electrical (electrodes charges) degrees of freedom. A preliminary analysis of the resulting equations of motion was performed and indicates that simultaneous active and passive damping using APPN is possible

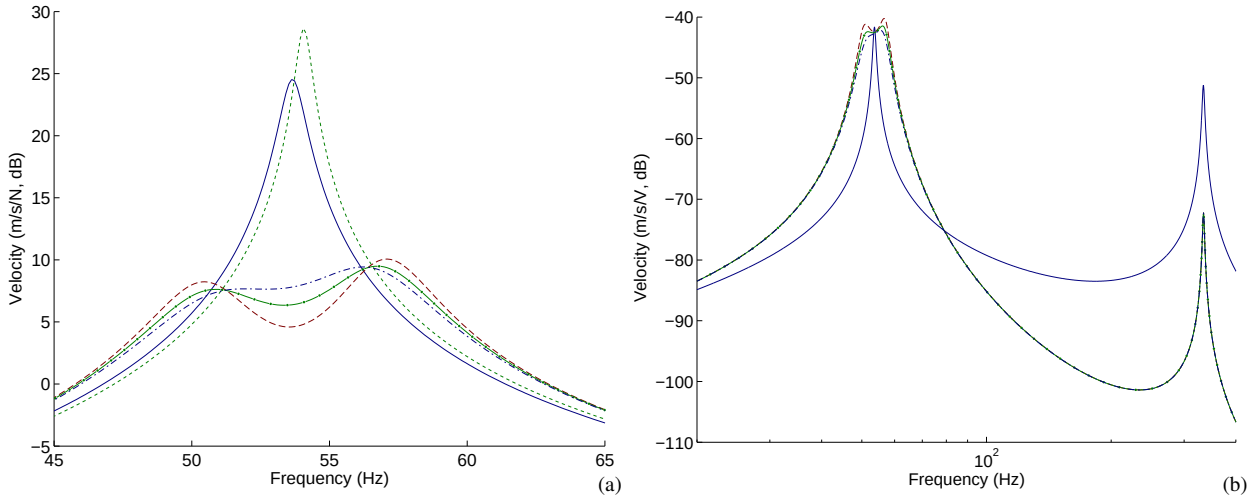

Figure 2. Beam tip velocity response (extension piezoceramic) induced by mechanical (a) and electrical (b) load. Electric circuit configuration - - -: open circuit; — : resistive (R=92.233 kΩ); – – : resonant (R=27.614 kΩ, L=691.413 H); – . – : resonant (R=41.422 kΩ, L=691.413 H); –o– : resonant (R=34.518 kΩ, L=691.413 H).

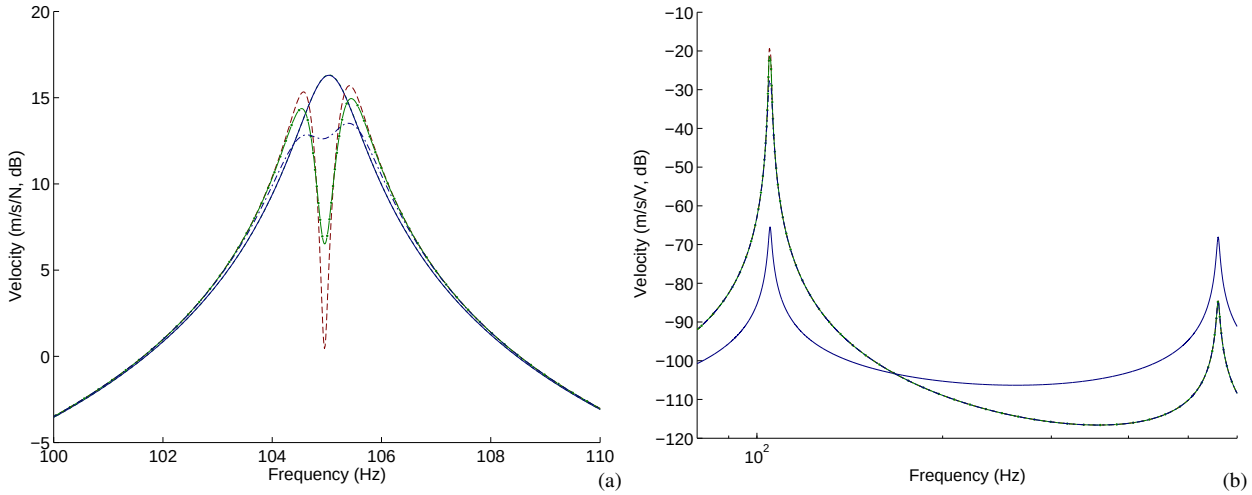

Figure 3. Beam tip velocity response (shear piezoceramic) induced by mechanical (a) and electrical (b) load. Electric circuit configuration - - -: open circuit; — : resistive (R=59.275 kΩ); – – : resonant (R=83.583 Ω, L=121.707 H); – . – : resonant (R=835.834 Ω, L=121.707 H); –o– : resonant (R=208.959 Ω, L=121.707 H).

and could be optimized by properly tuning the passive circuit components and by maximizing the electromechanical coupling. A preliminary numerical analysis has shown that both extension and shear APPN configurations can be very interesting since the passive damping can be combined with the increase of active control authority. Future works will focus on the optimization of the active-passive damping performance using extension, shear and combined extension-shear piezoelectric patches.

8. ACKNOWLEDGEMENTS

This research was supported by FAPESP and CNPq, through research grants 04/10255-7 and 473105/2004-7, which the authors gratefully acknowledge. The first author also acknowledges CNPq for a graduate scholarship.

9. REFERENCES

Baillargeon, B.P. and Vel, S.S., 2005, "Active vibration suppression of sandwich beams using piezoelectric shear actuators: experiments and numerical simulations," Journal of Intelligent Materials Systems and Structures, Vol. 16, No. 6, pp.517-530.

Benjeddou, A., 2006, "Shear-mode piezoceramic advanced materials and structures: a state of the art," to appear in Mechanics of Advanced Materials and Structures.

Benjeddou, A. and Ranger-Vieillard, J.-A., 2004, "Passive vibration damping using shunted shear-mode piezoceramics,"

In Topping, B.H.V. and Mota Soares, C.A., eds., Proceedings of the Seventh International Conference on Computational Structures Technology, Civil-Comp Press, Stirling, Scotland, p.4.

Benjeddou, A., Trindade, M.A., and Ohayon, R., 1999, "New shear actuated smart structure beam finite element," AIAA Journal, Vol. 37, No. 3, pp.378-383.

Forward, R.L., 1979, "Electronic damping of vibrations in optical structures," Applied Optics, Vol. 18, No. 5, pp.690-697.

Hagood, N.W. and von Flotow, A., 1991, "Damping of structural vibrations with piezoelectric materials and passive electrical networks," Journal of Sound and Vibration, Vol. 146, No. 2, pp.243-268.

Raja, S., Prathap, G., and Sinha, P.K., 2002, "Active vibration control of composite sandwich beams with piezoelectric extension-bending and shear actuators," Smart Materials and Structures, Vol. 11, No. 1, pp.63-71.

Sun, C.T. and Zhang, X.D., 1995, "Use of thickness-shear mode in adaptive sandwich structures," Smart Materials and Structures, Vol. 4, No. 3, pp.202-206.

Thornburgh, R.P., and Chattopadhyay, A., 2003, "Modeling and optimization of passively damped adaptive composite structures," Journal of Intelligent Materials Systems and Structures, Vol. 14, No. 4-5, pp.247-256.

Trindade, M.A., Benjeddou, A., and Ohayon, R., 1999, "Parametric analysis of the vibration control of sandwich beams through shear-based piezoelectric actuation," Journal of Intelligent Materials Systems and Structures, Vol. 10, No. 5, pp.377-385.

Trindade, M.A. and Maio, C.E.B., 2006, "Passive vibration control of sandwich beams using shunted shear piezoelectric actuators," in IV Congresso Nacional de Engenharia Mecânica, Recife, ABCM.

Tsai, M.S., and Wang, K.W., 1999, "On the structural damping characteristics of active piezoelectric actuators with passive shunt," Journal of Sound and Vibration, Vol. 221, No. 1, pp.1-22.

10. RESPONSIBILITY NOTICE

The authors are the only responsible for the printed material included in this paper.